Agricultural Water Management 303 (2024) 109027

Contents lists available at ScienceDirect

Agricultural Water Management

journal homepage: www.elsevier.com/locate/agwat

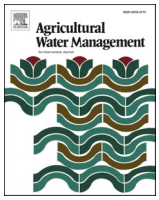

Water productivity in *Vitis vinifera* L. cv. Alvarinho using dual crop coefficient approach

Simão P. Silva [a,c], M. Isabel Valín [a], Susana Mendes [a], Claúdio Araujo-Paredes [b], Javier J. Cancela [c,*]

[a] Center for Research and Development, in Agrifood Systems and Sustainability (CISAS), Escola Superior Agrária, Instituto Politécnico de Viana do Castelo, Rua Escola Industrial e Comercial de NunÁlvares, Viana do Castelo 4900-347, Portugal
[b] Research Unit in Materials, Energy and Environment for Sustainability (PROMETHEUS), Escola Superior Agrária, Instituto Politécnico de Viana do Castelo, Rua Escola Industrial e Comercial de NunÁlvares, Viana do Castelo 4900-347, Portugal
[c] GI-1716 Projects and Planification, Agroforestry Engineering Department, Escuela Politécnica Superior de Ingeniería Lugo, University of Santiago de Compostela, Spain

ARTICLE INFO

Handling Editor: Dr Z Xiying

Keywords:
Cover crop
Crop water deficit, Crop water requirement modelling
Deficit irrigation
Soil water content
Water stress
SIMDualKc

ABSTRACT

Water productivity (WP) measurement determines the efficiency of water use by assessing the ratio of the crop yield to the amount of water used in production. The objective of this study was to identify the optimal irrigation treatment for *Vitis vinifera* L. cv. Alvarinho with ground cover in Northern Portugal, with a focus on water productivity. Two irrigation treatments (full irrigation—FI; deficit irrigation—DI) and a control (rainfed—R) were considered. The FI strategy represented the standard irrigation carried out by the vinegrower, based on the water availability and their experience. The cover crop was a variable factor, evaluated in terms of both height and density, both within the crop row and between the rows. In each of the treatments, the available soil water content (ASW) was measured in eight locations in the field throughout the growing season using a capacitive probe (Diviner 2000) previously calibrated. These measurements were used to calibrate the SIMDualKc model, which employed the dual crop coefficient approach. The successful calibration of the model, carried out with treatment R in 2018, was evidenced by the strong correlation between the ASW measured through the capacitive probe and that simulated by SIMDualKc (b=0.988 and r^2=0.995). After the model's calibration, the separation between the transpiration and evaporation components was determined. The maximum transpiration during the growing season was observed in the full irrigation treatment. In this context, the study proceeded to apply the soil water balance components and transpiration generated by the model in the calculation of the WP. The fruit yield productivity was determined by accounting for the total water use in the growing season. The total water used was calculated by combining the volumes of water applied for irrigation and precipitation and the soil water extracted during the growing season by crops and cover crops. The deficit irrigation strategy showed the best performance in both years, with WP values of 3.31 and 1.81 kg m^{-3} for the years 2018 and 2019, respectively. Therefore, the study concluded that deficit irrigation proved to be the most effective irrigation strategy in terms of water productivity and crop water use efficiency (WUE_c).

1. Introduction

Water plays a crucial role in agricultural production as a valuable resource, with this sector accounting for the majority of water withdrawals, representing approximately 70 % of the total worldwide water consumption. However, given the challenges posed by climate change, there is an inevitable need to curtail this consumption through the implementation of efficient water management practices (Fischer et al., 2007; Bwambale et al., 2022). To safeguard the future of this essential resource, it is imperative to foster sustainability in water use across all sectors, with a particular emphasis on agriculture (Brown et al., 2011; FAO and WWC, 2015). Precision irrigation can improve the sustainability of water usage by employing equipment and sensors such as soil water sensors (Beyá-Marshall et al., 2022), pressure chambers (Lakso et al., 2022), meteorological weather stations (Djaman et al., 2018) and drones (Araújo-Paredes et al., 2022). These technologies enable the collection of crucial data for irrigation decision-making, including the soil water content, leaf water potential, evapotranspiration and

* Corresponding author.
E-mail address: javierjose.cancela@usc.es (J.J. Cancela).

https://doi.org/10.1016/j.agwat.2024.109027
Received 13 February 2024; Received in revised form 19 August 2024; Accepted 20 August 2024
Available online 26 August 2024

normalized vegetation index. This approach significantly reduces water wastage and improves the overall efficiency (Acevedo-Opazo et al., 2010 and González Perea et al., 2018). Precision irrigation is becoming crucial to address climate change. Although certain aspects of climate change, such as increased precipitation, may offer localized benefits, there are also adverse impacts, including reduced water availability and more frequent extreme weather events (Alcamo et al., 2007; Iglesias and Garrote, 2015). Given that climate change is recognized as one of the most significant environmental challenges of this century (KPMG International, 2012), there is a need to evaluate the impact and efficiency of water use in the agricultural sector (Civit et al., 2018; Chen et al., 2023; Fatichi et al., 2023).

To evaluate the water efficiency in agriculture, the water productivity (WP) and crop water use efficiency (WUE_c) methods are frequently employed (Junquera et al., 2012; Trout and DeJonge, 2017; Fatichi et al., 2023). The WP is expressed as the ratio between the yield and the water used or between the value of the product and the water used. The optimal WP outcome is attained by reducing the water consumption per unit of grape production, provided that it does not compromise other factors, such as quality (Rodrigues and Pereira, 2009; Pereira et al., 2020a; Fernández, 2023). The WP has been employed as a tool for water management in various crops, including wheat, maize and potatoes (Zhang et al., 2021), apples (Zhou et al., 2023) and olives (Fernández et al., 2020) and in the Atlantic viticulture (Buesa et al., 2017; Soltekin et al., 2020). In addition, the crop density and training system have been reported as factors influencing the WP, as well as crop evapotranspiration, in various crops, such as apple (Jiang and He, 2021) and grapevine (Yuste et al., 2004; Prieto et al., 2020). Several studies suggest that the application of deficit irrigation strategies has a positive impact on water productivity and can also improve the quality of grapes (Shellie, 2014; Phogat et al., 2017; Ma et al., 2023).

To ensure efficient water use, a comprehensive understanding of the actual crop water requirements, including the crop evapotranspiration during the crop season, is crucial (Allen et al., 1998; Fatichi et al., 2023). As mentioned by Fernández (2023), the terms crop water use efficiency (WUE_c) and water productivity (WP) are often confused; for this reason, the correct definition of a numerator and denominator is required (Pereira et al., 2020). To calculate the WUE_c, the numerator should contain the actual crop evapotranspiration and the denominator should contain the sum of the irrigation applied and the total precipitation during the season.

The actual crop evapotranspiration can be obtained using the dual crop coefficient approach (Allen et al., 1998). This approach has already been applied to several crops (Rosa et al., 2012a; Rallo et al., 2021; Silva et al., 2021). The actual crop evapotranspiration ($ET_{c\ act}$) is determined using Eq. (1), which incorporates the actual crop coefficient ($K_{cb\ act}$) (Allen et al., 1998; Pereira et al., 2021a).

$$ET_{c\ act} = (K_s K_{cb} + K_e) ET_o = K_{c\ act} \times ET_o \quad (1)$$

where $ET_{c\ act}$ represents the actual crop evapotranspiration; K_s represents the water stress coefficient, ranging between 0 and 1.0; K_{cb} represents the basal crop coefficient; K_e is the soil evaporation coefficient; ET_o represents the reference evapotranspiration; and $K_{c\ act}$ is the actual crop coefficient.

The total evapotranspiration is determined via the water requirements for crop growth ($K_{cb\ crop}$), the establishment of ground cover vegetation ($K_{cb\ gcover}$) and soil evaporation (Allen and Pereira, 2009; Fandiño et al., 2012). In the 'Vinhos Verdes' region, ground cover vegetation (GCV) persists throughout the entire season, with variations in height and density during the growing season, leading to variations in the cover crop coefficient ($K_{cb\ gcover}$) (Afonso et al., 2003; Silva et al., 2021). Active ground cover requires water but is sustainable if the many ecosystem services provided by the cover crops in the vineyards are taken into account (Garcia et al., 2018).

In order to accurately include all indicators involved in the growing process and obtain the soil water balance, numerous studies have used models such as the SIMDualKc model (Rosa et al., 2012b; Pereira et al., 2020a), SALTMED model (Ragab, 2002; El-Sadek, 2014) and AquaCrop model (González Perea et al., 2018; Er-Raki et al., 2021). These software programs were considered accurate and precise in their inclusion of multifactorial factors, including all variables related to the soil, plant, climate, irrigation and soil cover. The SimDualKc model incorporates information on the soil, climate, crops and cover crops both within and between vine rows. The model outputs several variables that can be used to derive indicators, including the total growing season water use, actual crop evapotranspiration and total transpiration (Rosa et al., 2012b; Pereira et al., 2020a), allowing the accurate calculation of the water productivity (WP) and crop water use efficiency (WUE_c).

The aim of this study is to give an insight into the water productivity of *Vitis vinifera* cv. Alvarinho, trained in a vertical shoot system with a low density, in Northwestern Portugal. To achieve this, the study implements the dual Kc approach using the SIMDualKc model, applying this approach to different irrigation strategies, to verify an increase in water productivity and water use efficiency in cv. Alvarinho. The purpose of this research is to support irrigation management programs that improve the water use efficiency in agriculture, with a specific emphasis on vineyards.

2. Materials and methods

2.1. Study area

The study was carried out over two growing seasons (2018 and 2019) in a commercial cv. Alvarinho vineyard located in Monção, Northwestern Portugal (42°04'39.3"N 8°21'31.0"W and 175 m.a.s.l.). The vineyard, which totalled 1.9 ha, was planted in 2009 with row spacing of 3.0 m and vine spacing of 3.0 m (1111 plants ha^{-1}). It was trained in a north–south orientation, with a 31.5 ° slope to the west, using a vertical shoot system (Fig. C.1). The irrigation system utilized drip irrigation, with a surface drip line in vineyard rows at 0.40 m above the soil and pressure-compensated emitters (4 L h^{-1}) at intervals of 1 m (Fig. D.1). In May 2018, a field experiment was conducted to evaluate the irrigation performance, obtaining distribution uniformity (DU) of 91 % (Merriam and Keller, 1978). For the detailed definitions of all parameters, please refer to Appendix A.

2.1.1. Climate and meteorological description

The climate of the study area was classified as Atlantic, with relatively mild summers and annual rainfall above 1200 mm (Fraga et al., 2014). The Köppen–Geiger classification for the area was Csb (Kottek et al., 2006).

The weather station located in the field (UNL Ameriflux Site, Mead NE) collected daily meteorological data, including the temperature (°C), humidity (%), wind speed at 2 m height (m s^{-1}), shortwave radiation (MJ m^{-2} d^{-1})) and precipitation (mm). The reference evapotranspiration (ET_o) was calculated using the FAO Penman–Monteith equation (Allen et al., 1998) (Eq. (2)). Throughout the growing season, in 2018, the ET_o, ranged between 1.1 (DOY 96) and 8.1 (DOY169) mm day^{-1}; in 2019, it ranged between 1.5 (DOY94) and 7.0 (DOY151) mm day^{-1} (Fig. 1). The daily variability was high, depending on factors such as the net radiation, temperature and wind speed.

$$ET_o = \frac{0.408\Delta(R_n - G) + \gamma \frac{900}{T+273} U_2 (e_s - e_a)}{\Delta + \gamma\ (1\text{-}0.34U_2)} \quad (2)$$

where Δ represents the slope of the saturation vapor pressure–temperature relationship at the mean air temperature (kPa $°C^{-1}$), Rn is the net radiation at the crop surface (MJ m^{-2} d^{-1}), G is the soil heat flux density (MJ m^{-2} d^{-1}), γ is the psychometric constant (kPa $°C^{-1}$), T is the mean daily air temperature (°C), U_2 is the wind speed (m s^{-1}) at 2 m height and (e_s− e_a) represents the vapor pressure at 2 m (kPa) (e_s is

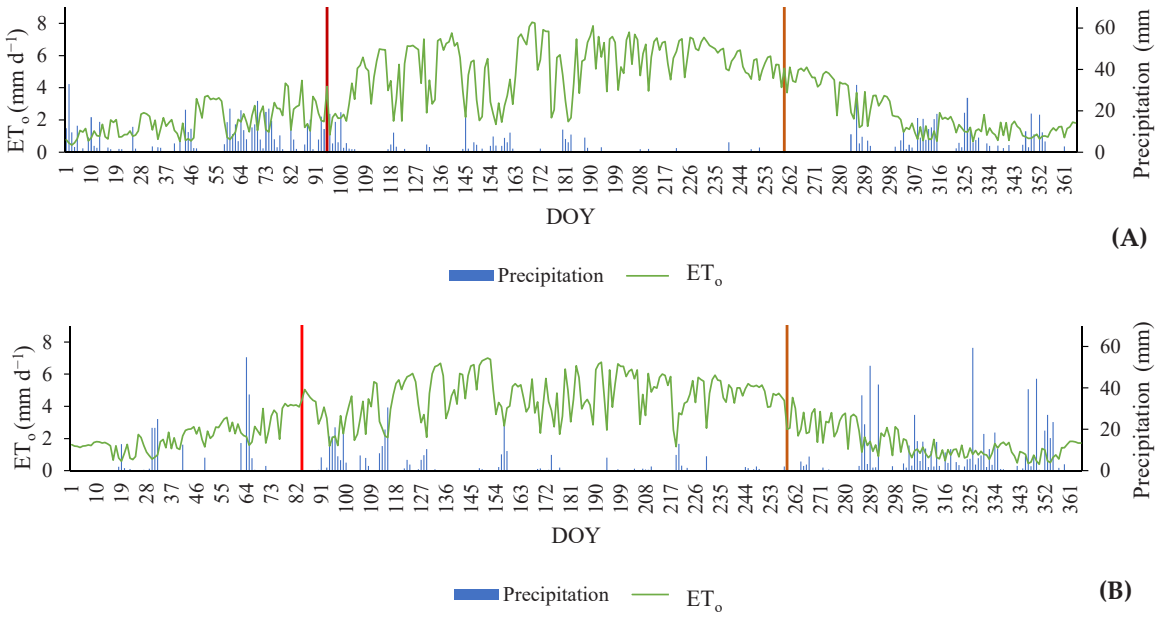

Fig. 1. Precipitation (mm) and reference evapotranspiration (ET_o, mm d^{-1}) for 2018 (A) and 2019 (B). The vertical bars represent the beginning (|) and end (|) of the growing season.

saturated and e_a is the actual vapor pressure).

In 2018 and 2019, the total rainfall was 1126 and 1231 mm, respectively. The growing season lasted from DOY95 to DOY260 in 2018 and from DOY84 to DOY259 in 2019. Within the growing season, the rainfall amount was 228 mm and 332 mm for 2018 and 2019, respectively (Fig. 1). The average temperature in 2018 was 19.1 ℃, while, in 2019, it was 18.4 ℃.

2.1.2. Soil and active ground cover characterization

The soil texture was sandy loam, composed of 67.2 % sand, 16.4 % silt and 16.4 % clay, with 1.74 % organic matter. The total available water (TAW) was calculated using Eq. (3) and was in agreement with that reported for other similar soil and cultivars (Cancela et al., 2016; Silva et al., 2021). The TAW result was 112.8 mm considering a depth root (Z_r) of 0.8 m, similar to that stated by Silva et al. (2021) for grapevines. Nine undisturbed soil samples of 100 cm^3 were collected from three sites at depths of 0–20 cm, 20–50 cm and 50–80 cm, to determine the soil water retention characteristics. In the laboratory, the field capacity was determined by using a pressure plate to apply suction of −33 kPa to the saturated soil samples. The wilting point was obtained using the same samples, with suction of −1500 kPa (Evett et al., 2019). The average field capacity (FC) of the samples was 0.281 $cm^3\ cm^{-3}$, and the average wilting point (WP) was 0.140 $cm^3\ cm^{-3}$, up to a depth of 0.8 m.

$$TAW = 1000 * Z_r(FC - WP) \quad (3)$$

where Z_r is the depth root, FC is the field capacity and WP is the wilting point.

The active ground cover, consisting of spontaneous species with most plants belonging to the Poaceae family, was photographed during the growing season with a digital camera (Canon EOS 77D, JP) and subsequently characterized in terms of height and density. Eight observations in 2018 and thirteen observations in 2019 were used to characterize the cover crop at different growth stages (Appendix B). The density of the vegetation varied over time due to mowing, ranging from 50 % to 95 % within rows and 10–90 % between rows. The height of the ground cover crop also varied, measuring between 0.05 m and 0.2 m within rows and 0.03 m and 0.18 m between them.

2.2. Experimental design

Two irrigation strategies and a control were implemented in the study. The full irrigation (FI) treatment represented the irrigation applied by the vinegrower, which was dependent on the water availability and the vinegrower's experience. The deficit irrigation (DI) treatment was designed to provide half the volume of the FI treatment. The control treatment was rainfed (R), the most common method practiced in the region. Each treatment comprised two replicates with four vineyard rows each. Access probes were installed in the two central rows, while the other two rows served as buffers (Fig. D.1). To ensure a homogeneous test area, the apparent electrical conductivity of the soil (EC_a) was assessed (Mirás-Avalos et al., 2020). Data were collected on 5 April 2018 at 1419 points using an EM38 instrument (Geonics Ltd., CA), a field computer and a GPS RTK for georeferencing. The EM38 instrument's transmitter–receiver coils were oriented parallel to the Earth in vertical dipole, an effective mode for deeper investigation (1.50 m) (Nadler, 1982). The ECa, calculated with the actual soil temperature, was adjusted to 25 ºC using the soil temperature measured every 5 minutes at a depth of 0.25 m with four temperature probes (Fig. C.1).

The available soil water content (ASW, mm) data were obtained by converting the soil moisture values obtained with a capacitive probe, previously calibrated following the instructions provided in the manufacturer's manual (Diviner 2000, Sentek, AU). Twenty-four access probe tubes were installed only in the rows, because this was the location where the vineyard extracted the majority of the water (Fandiño et al., 2012; Pagay, 2022), at eight soil depths every 10 cm and up to 80 cm (Silva et al., 2021), distributed across the treatments (eight access probe tubes per treatment). The access probes were installed one meter from the plant and between two emitters (Fig. D.1). Irrigation was started in both years after the volumetric soil moisture content had reached 70 % of the field capacity. In the 2018 season, irrigation was carried out between DOY 211 and DOY 243. Nine irrigation events resulted in 103 mm for the FI treatment and 58 mm for the DI treatment. In 2019, irrigation was carried out between DOY 211 and DOY 243. The FI treatment received 75 mm of water through seven irrigation events, while the DI treatment received 40 mm of water through the same number of irrigation events.

Phenological developments were assessed using the Baggiolini scale

(Baggiolini et al., 1993), which was later adapted to our FAO standard crop growth stages (Allen et al., 1998) (Table 1). The crop heights (h) and the fraction of soil shaded by the crop (f_c) were visually observed at solar noon and monitored during the entire growing season. The dates of the crop growth stages are presented in Table 1.

2.3. Model calibration and validation

The DualKc approach employs a set of equations, presented in Table 2. The SIMDualKc model was used to calculate the evapotranspiration (ET_c) using the dual crop coefficient approach (Allen et al., 1998) with a daily time step through equation (4). In this approach, the capillary rise (CR) and deep percolation (DP) were calculated using the parametric equations described by Liu et al. (2006) and employing a curve number of 60 to calculate the surface runoff (Rosa et al., 2012a, b).

The model calculates the $ET_{c\ act}$ (Eq. (1)) based on the soil water available within the root zone, using a water stress coefficient (K_s, 0–1). K_s is calculated daily as a linear function of the depletion of the available water in the effective root zone, as shown in equations (5) and (6). The amount of energy available at the soil surface, in combination with the energy consumed for crop transpiration, limits the evaporation from the soil surface (Allen et al., 1998).

The model computes the soil evaporation coefficient (K_e) using the daily water balance of the soil layer via equation (7). To calculate K_e, it is necessary to determine the exposed and wetted soil fraction (f_{ew}) (equation (8) and the soil evaporation reduction coefficient (K_r). K_r is calculated using the two-stage drying cycle approach (Allen et al., 1998), where the first stage (9) is the energy-limiting stage and the second is the water-limited stage or falling rate stage (10). Furthermore, the initial values of the basal crop coefficients ($K_{cb\ ini}$, $K_{cb\ mid}$ and $K_{cb\ end}$) were derived from the observed ground cover fraction (f_c) and plant height values (Table 1) using equation (11) proposed by Allen and Pereira (2009). The density coefficient (K_d), $K_{cb\ full}$ and stomatal adjustment (F_r) were estimated using equations (12), (13) and (14), respectively (Allen and Pereira, 2009).

Then, the calibration of the model was required (Fandiño et al., 2012; Rosa et al., 2012a; Paredes et al., 2018; Darouich et al., 2023), which involved adjusting the following crop parameters: the initial basal crop coefficient ($K_{cb\ full\ ini}$), the midseason basal crop coefficient ($K_{cb\ full\ mid}$), the end basal crop coefficient ($K_{cb\ full\ end}$), and the p depletion fractions. $K_{cb\ full}$ was used to determine the basal K_{cb} expected for vegetation under full cover conditions, as verified in our study vineyard.

The soil evaporation parameters, including the evaporable layer depth ($Z_e = 0.10$ m), total evaporable water (TEW) and readily evaporable water (REW), were obtained through the soil characteristics under the local conditions of cv. Alvarinho. The total evaporable water (TEW) used was 21 mm, while the readily evaporable water (REW) used was 9 mm and the depth of the soil evaporation layer (Ze) was 0.1 m.

The F_r values used in this work for the crop were 0.21, 0.46 and 0.20 for the early, mid- and end seasons, respectively, with an ML of 1.5. A ground cover F_r value of 0.25 was used in this work. Information about variations in the density and height of the cover crop in the rows and inter-row areas (Appendix B) was included in the software to ensure that the model accounted for the water used by the cover crop.

Equations 4–10 were defined by Allen et al. (1998) and equations 11–14 were defined by Allen and Pereira (2009).

For calibration, the differences between the observed and simulated ASW values were minimized in the R treatment for 2018. The other treatments (2018-DI, 2018FI, 2019-R, 2019-DI and 2019-FI) were used for validation purposes. Treatment R 2018 was selected for calibration due to its a broad range of ASW and the absence of irrigation events, which could potentially introduce bias. The calibration process began with the reference $K_{cb\ full}$,Fr, p and ML parameters, and subsequent adjustments were made.

The methodology used to assess the model's accuracy was similar to that used in earlier studies (Silva et al., 2021). Linear regression was performed by comparing the observed and simulated ASW values, with the regression forced to the origin (Pereira et al., 2020b). A set of goodness-of-fit indicators was used to evaluate the model's performance during calibration and to assess the validation results. The indicators included the regression coefficient (b), determination coefficient (r^2), root mean square error (RMSE, mm) (see Eq. (15)), normalized RMSE (NRMSE, %), average relative error, percent bias of estimation (PBIAS, %) (see Eq. (16)), modelling efficiency (EF, dimensionless) (see Eq. (17)), average absolute error (AAE, mm) (see Eq. (18)) and index of agreement (dIA, dimensionless) (see Eq. (19)) between the observed and model-predicted values, respectively (Oi and Pi (i = 1, 2,…, n)).

$$RMSE = \left[\frac{\sum_{i=1}^{n}(P_i - O_i)^2}{n}\right]^{0.5} \quad (15)$$

$$PBIAS = 100 \quad \frac{\sum_{i=1}^{(n}(O_i - P_i)}{\sum_{i=1}^{(n}(O_i} \quad (16)$$

$$EF = 1.0 - \frac{\sum_{i=1}^{(n}(O_i - P_i)^2}{\sum_{i=1}^{(n}(O_i - \overline{O})^2} \quad (17)$$

$$AAE = \frac{1}{n}\sum_{i=1}^{n}|O_i - P_i| \quad (18)$$

$$dIA = 1.0 - \frac{\sum_{i=1}^{n}(P_i - O_i)^2}{\sum_{i=1}^{n}(|P_i - \overline{O}| + |O_i - \overline{O}|)^2} \quad (19)$$

The calibration of the $K_{cb\ full}$, p, Fr and ML parameters involved analysing and improving the regression coefficient (b) and determination coefficient (r^2) parameters between the observed and simulated ASW, aligning them closer to 1. The b and r^2 indicators are two related but different correlation measures. In this case, a higher r^2 value indicates a stronger correlation between the obtained and simulated values, even if they are not identical. Conversely, b is a performance indicator, with a value closer to 1 indicating lower volatility between the observed and simulated values.

Then, the RMSE was used to measure the average difference between the predicted values from the model and the observed ones. The PBIAS was used to assess the average tendency of the simulated values to be higher or lower than the observed values. The AAE represents the mean absolute error between the simulated and observed values. The aim of calibration/validation was to minimize these indicators (RMSE, PBIAS and AAE) and bring them closer to zero, in line with Rosa et al. (2012a). The aim was to achieve values close to 1 for the EF and dIA indicators. This is because an EF close to 1 indicates a direct relationship between the real and simulated values, while a dIA value close to 1 indicates a balanced ratio between the mean squared error and the potential error.

Table 1
The vineyard crop growth stage, height (h) and fraction of the soil covered by the crop in the vineyard (fc) on respective days of the year (DOY).

Crop Growth Stage (Allen et al. 1998)	Baggiolini scale (Baggiolini et al. 1993)	DOY in 2018	DOY in 2019	h (m)	f_c
Initiation	C (green-tip bud burst)	95	84	0.6	0.01
Start of rapid growth	D (leaf emergence)	110	106	0.8	0.05
Start of midseason	I (flowering)	150	147	1.5	0.10
Start of maturity	M (veraison)	214	206	1.8	0.20
Harvesting	N (maturity)	260	259	1.8	0.20

Table 2
The equations used to perform the DualKc approach.

Equation		Terms
$D_{r,i} = D_{r,i-1} - (P - RO)_i - I_i - CR_i + ET_{c,i} + DP_i$	(4)	$D_{r,i}$ and $D_{r,i-1}$ represent the root zone depletion, in mm, at the end of day i and i − 1, respectively; P_i is the precipitation; R_{Oi} is the runoff; I_i represents the net irrigation depth; CR_i is the capillary rise from the groundwater table; $ET_{c;i}$ is the crop evapotranspiration; and DP_i is deep percolation, referring to the end of day (i) or the end of the previous day (i – 1), and all are expressed in mm.
$Ks = \frac{TAW - D_r}{TAW - RAW} \rightarrow for D_r > RAW,\ (RAW = p * TAW)$	(5)	TAW and RAW are, respectively, the total and readily available soil water (mm) relative to the root zone depth (Zr); p is the soil water depletion fraction for no stress.
$Ks = 1 \rightarrow for D_r \leq RAW$	(6)	
$K_e = K_r(K_{cmax} - K_{cb}) \rightarrow with K_e \leq f_{ew} K_{cmax}$	(7)	$K_{c\ max}$ is the maximum value of K_c following a wetting event by rain or irrigation, generally 1.20, and f_{ew} is the fraction of the soil that is both exposed to radiation and wetted by rain or irrigation, i.e., the fraction of the soil surface from which most evaporation occurs.
$f_{ew} = \min(1 - f_c, f_w)$	(8)	f_c represents the fraction of the ground covered by the crop and f_w is the fraction of soil wetted by irrigation.
$Kr = 1 \rightarrow for D_{e,i-1} \leq REW$	(9)	De,i−1 is the cumulative depth of evaporation (depletion) from the soil surface layer at the end of day i−1. TEW represents the maximum cumulative depth of evaporation (depletion) from the soil surface layer and REW is the readily evaporable water.
$Kr = \frac{TEW - D_{e,i-1}}{TEW - REW} \rightarrow for D_{e,i-1} > REW$	(10)	
$K_{cb} = K_{cmin} + K_d(K_{cb\ full} - K_{cmin}),\quad K_{c\ min}=0.15$	(11)	$K_{c\ min}$ is the minimum basal K_c for bare soil, with $K_{c\ min} = 0.15$ in typical agricultural conditions and for native vegetation when the frequency of rainfall is high; K_d represents the density coefficient; $K_{cb\ full}$ is the K_{cb} estimated during peak plant growth for conditions with almost total soil cover (or LAI > 3).
$K_d = \min\left(1,\ M_L f_{c\ eff}, f_{c\ eff}^{\left(\frac{1}{1+h}\right)}\right)$	(12)	$f_{c\ eff}$ is the effective fraction of ground covered or shaded by vegetation [0.01–1] at solar noon; M_L is a multiplier of $f_{c\ eff}$ describing the effect of the canopy density on the shading and on the maximum relative evapotranspiration per fraction of shaded ground [1.5–2.0].
$K_{cb\ full} = F_r\left(\min(1.0 + k_h h,\ 1.20) + [0.04(u_2 - 2) - 0.004(RH_{min} - 45)]\left(\frac{h}{3}\right)^{0.3}\right)$	(13)	F_r represents the resistance correction factor; the sum $(1 + k_h\ h)$ represents the effect of the crop height; u_2 is the average daily wind speed (m s^{-1}) at a height of 2 m above ground level; RH_{min} (%) is the average daily minimum relative humidity during the growth period; and h is the mean plant height (m) during the mid-season.
$F_r = \frac{\Delta + \gamma(1 + 0.34u_2)}{\Delta + \gamma(1 + 0.34u_2\frac{r_l}{r_{typ}})}$	(14)	Δ is the slope of the saturation vapor pressure vs. air temperature curve, kPa $°C^{-1}$; γ is the psychrometric constant, kPa $°C^{-1}$; u_2 is the average daily wind speed (m s^{-1}) at a height of 2 m above ground level; and r_l and r_{typ} are, respectively, the mean leaf resistance and the typical leaf resistance (s m^{-1}) for the vegetation in question. The original version of this equation was established with a fixed $r_{typ} = 100$ s m^{-1}, a common value for annual crops, but the default F_r values were recently reviewed for trees and vines and several annual crops (Pereira et al. 2021b).

After calibration, it was confirmed that the simulated values obtained through the SIMDualKc model were similar to the average values of the available soil water (ASW) obtained with the capacitive probes. The validation process utilized previously calibrated parameters from other treatments during 2018 and 2019.

Obtaining good calibration and respective validation was crucial to support the accuracy of the model in performing the ASW evaluation. In the present study, this was also important because other variables provided by the model were used, such as the transpiration crop plus ground cover (T, m^3 ha^{-1}), actual crop evapotranspiration ($ET_{c\ act}$, m^3 ha^{-1}), total water used (TWU, mm), actual basal crop coefficient ($K_{cb\ (gcover + crop)\ act}$), soil evaporation coefficient (K_e), water stress coefficient (K_s) and ground cover basal crop coefficient ($K_{cb\ gcover}$) during the growing season for all treatments in both years. The TWU is achieved by combining the results of irrigation, precipitation and the water removed from the soil during the growing season. The amount of water extracted from the soil is calculated by subtracting the initial soil moisture content from the final value obtained through the model.

2.4. Water productivity and water use efficiency

To determine the effects of deficit irrigation strategies, several water indices (WP and WUE_c) were determined, whose requirements included the yield and biomass production. Therefore, harvesting and pruning were carried out on the same plants, resulting in four groups of seven plants (28 plants) for each treatment (DI and FI) and in the control (R), totalling 84 plants. Each plant was harvested individually to determine the production of the plant, which was later converted into a yield (kg ha^{-1}). The same set of plants was selected for pruning and the weight of the wood was measured individually to obtain the pruning wood indicator (kg ha^{-1}).

The water productivity in viticulture, WP (kg m^{-3}), was defined as the ratio between the vineyard fruit yield, FY (kg ha^{-1}), and the total water use, TWU (m^3 ha^{-1}), as shown in Eq. (20). Recognizing the significant water usage associated with grapevine vegetative growth, two new indices were introduced by Cancela et al. (2016) to incorporate the pruning wood and the fruit yield plus the pruning weight (Eqs. (21) and (22)). Another way to demonstrate the water productivity is to compare the fruit yield with the transpiration (T) (Eq. (23)) or actual crop evapotranspiration ($ET_{c\ act}$) (Eq. (24)) during the growing season (Pereira et al., 2020). Finally, the crop water use efficiency (WUE_c) was estimated by applying the concept defined by Fernández (2023), using Eq. (25).

$$WP_{FY} = \frac{FY}{TWU} \tag{20}$$

$$WP_{PW} = \frac{PW}{TWU} \tag{21}$$

$$WP_{FY+PW} = \frac{FY + PW}{TWU} \tag{22}$$

$$WP_T = \frac{FY}{T} \tag{23}$$

$$WP_{ETc} = \frac{FY}{ETc\ act} \tag{24}$$

$$WUE_c = \frac{ETc\ act}{I + P} \tag{25}$$

where TWU corresponds to the water used to achieve the FY (m^3 ha^{-1}), PW refers to the pruning wood (kg ha^{-1}), FY + PW is the sum of the fruit yield and pruning wood (kg ha^{-1}), T corresponds to transpiration (crop plus ground cover, m^3 ha^{-1}), $ET_{c\ act}$ is the actual crop

evapotranspiration ($m^3\ ha^{-1}$), I is the irrigation applied and P is the total precipitation during the season.

For the FY parameter, the production of 28 vines was considered in each treatment (84 vines per year). In this study, the PW was determined by individually weighing the pruning firewood from the same vines.

The TWU parameter was calculated considering the water used during the growing season, including both precipitation and irrigation, as proposed by other authors (Cancela et al., 2016; Gonzalez-Fernandez et al., 2020; Ma et al., 2023). The calculation also took into account the variation, represented as the difference in the ASW between the initiation and harvest stages (ΔASW), as shown in Eq. (26).

$$\Delta ASW = ASW_{initial} - ASW_{harvest} \quad (26)$$

where $ASW_{initial}$ and $ASW_{harvest}$ represent the available soil water at the initial and harvest stages, respectively.

2.5. Quality assurance, quality control and statistical analysis

To ensure quality assurance and quality control, the climate data were reviewed to minimize errors and biases in the system (Allen et al., 2011). To evaluate the data integrity, we followed the methodology proposed by Allen (1996) and then calculated the ET_o (Allen et al., 1998). The data were analysed and improved to reduce errors. Data from a meteorological station located 35 km away were used to replace atypical or missing data due to technical problems. This weather station was complementary because of its proximity. Precipitation values of approximately 0.01 mm, which were due to condensation, were eliminated. To analyse the variability in the treatment means and post hoc comparisons, a one-way ANOVA procedure in SPSS 27 was used. The post hoc tests used Duncan's method with a significance level of $p < 0.05$.

3. Results

The standard and calibrated crop parameters, $K_{cb\ full\ ini}$, $K_{cb\ full\ mid}$, $K_{cb\ full\ end}$ and p, are shown in Table 3(Allen et al., 1998; Allen and Pereira, 2009). The values for $K_{cb\ full\ mid}$ and $K_{cb\ full\ end}$ were slightly lower than those suggested by the standard. Furthermore, there was a slightly higher mean p-value compared to the standard.

The ASW results observed and simulated in R 2018 are presented in Fig. 2. The initial RAW value was 56.4 mm, which progressively decreased to 50.8 mm as the crop approached the mid-season. The value remained stable until the beginning of maturation, after which it decreased again to 45.1 mm at the final stage. A high level of agreement was found between the observed and simulated ASW values in all treatments, particularly in treatments without irrigation (R). Nevertheless, at certain points, there was a tendency towards overestimation and underestimation. The treatment described as FI-2018 (Fig. 2 A.3) exemplified a case of model overestimation starting from DOY 211, where a deviation between the observed and simulated values occurred. In 2019, the model overestimated the ASW of all treatments on DOY 199 (Fig. 2 B). A greater quantity of water was extracted from the soil in 2018 than in 2019 (Fig. 2). In the 2018 growing season, 192, 171 and 133 mm of soil water was removed from the soil in treatments R, DI and FI, respectively. In the 2019 growing season, 73, 36 and 6 mm of soil water was removed from the soil in treatments R, DI and FI, respectively.

Table 3
The standard and calibrated model parameters for cv. Alvarinho.

Parameter		Standard	Calibrated
$K_{cb\ full\ ini}$ (dimensionless)		0.20	0.22
$K_{cb\ full\ mid}$ (dimensionless)		0.80	0.53
$K_{cb\ full\ end}$ (dimensionless)		0.60	0.24
p_{ini} (dimensionless)		0.45	0.50
p_{mid} (dimensionless)		0.45	0.55
p_{end} (dimensionless)		0.45	0.60
Fr_{ini}		0.20–0.70	0.21
Fr_{mid}		0.65–0.70	0.46
Fr_{end}		0.50–53	0.20
ML		1.50	1.50
Capillary rise	a1	320.8	281
	b1	−0.16	−0.16
	a2	303.2	231.55
	b2	−0.54	−0.54
	a3	−0.15	−0.15
	b3	2.1	2.1
	a4	7.55	7.55
	b4	−2.03	−2.03
Deep percolation	a_D	390	400
	b_D	−0.0173	−0.0173

Standard (Allen et al., 1998; Allen and Pereira, 2009; Pereira et al., 2020b) K_{cb} = basal crop coefficients, p = depletion fraction,Fr = stomatal adjustment, ML = canopy transparency. Standard parameters for capillary rise and deep percolation were obtained according to Liu et al. (2006)Liu et al. (2006)

The results of the goodness-of-fit indicators used to evaluate the model fit during calibration and to assess the validation results are presented in Table 4. The underlined values in the table represent the calibration performed for the R-2018 treatment. The regression and determination coefficients (b and r^2) resulting from a forced regression to the origin are presented, along with the values of the indicators EF (Eq. 17), RMSE (Eq. 15), NRMSE (%), PBIAS (Eq. 16), dIA (Eq. 19) and AAE (Eq. 18). The calibration process (R-2018) provided the best values for the regression coefficient and the determination coefficient of 0.988 and 0.995, respectively.

The regression coefficient approached 1.0 (ranging from 0.952 to 1.044), indicating statistical similarity between the predicted and observed values for all treatments and crop seasons. The r^2 values ranged from 0.928 to 0.995, indicating that the model accounted for most of the total variance in the observed values. The low RMSE values, ranging from 4.320 to 5.384 mm, indicate that the estimation errors were small. These values, in conjunction with the low NRMSE (ranging from 4.764 % to 6.684 %), indicate low residual errors. The AAE values were also rather low, ranging between 3.835 mm and 4.800 mm, corresponding to values lower than 4.255 % of the TAW. The PBIAS was very low, suggesting an underestimation bias in the FI-2018 treatment (PBIAS = 5.386) and an overestimation bias (PBIAS = −4.503) in the DI-2019 treatment.

Differences were observed in all indicators used between the R-2018 treatment (calibration) and the validation treatments. The R-2018 values were found to be the most accurate, while the FI-2019 values were the least accurate. However, even in FI-2019, a b of 1.044 and an r^2 of 0.963 were observed, which are close to 1, indicating a high level of agreement between the observed and simulated ASW. Therefore, the model did not exhibit a trend of under- or overestimation bias, showing a slight underestimation in 2018 and a slight overestimation in 2019.

Variations in the different coefficients, namely K_e, $K_{cb\ full}$ and $K_{c\ act}$, were observed among the irrigation treatments (Fig. 3). Furthermore, the stress levels (K_s) for each treatment in both seasons are presented, with lower values observed in the R and DI treatments (Fig. 3). The values for the $K_{cb\ (gcover\ +\ crop)\ act}$ are presented in Table 5.

During the 2018 growing season, the active ground cover density in the rows varied between 50 % and 95 %, with the height varying between 0.05 and 0.18 m. In addition, the active cover density varied between 60 % and 90 % with a height within rows of between 0.05 m and 0.15 m (Fig. 4). In 2019, the density of the active ground cover in the rows ranged from 60 % to 90 %, with heights ranging from 0.06 m to 0.20 m (Fig. 4). Between the rows, the density ranged from 10–90 %, and the height ranged from 0.03 m to 0.18 m. Variations in height and density occurred in both years, mainly as a result of agronomic practices (phytosanitary treatments and vegetation cutting).

This variation was more intense in 2019 because, on DOY 146, a high level of vegetation cutting was carried out between the rows. The effect of the ground cover was different during the two growing seasons: the $K_{cb\ gcover}$ (simulated by SIMDualKc) in 2019 (ranging between 0.281 and

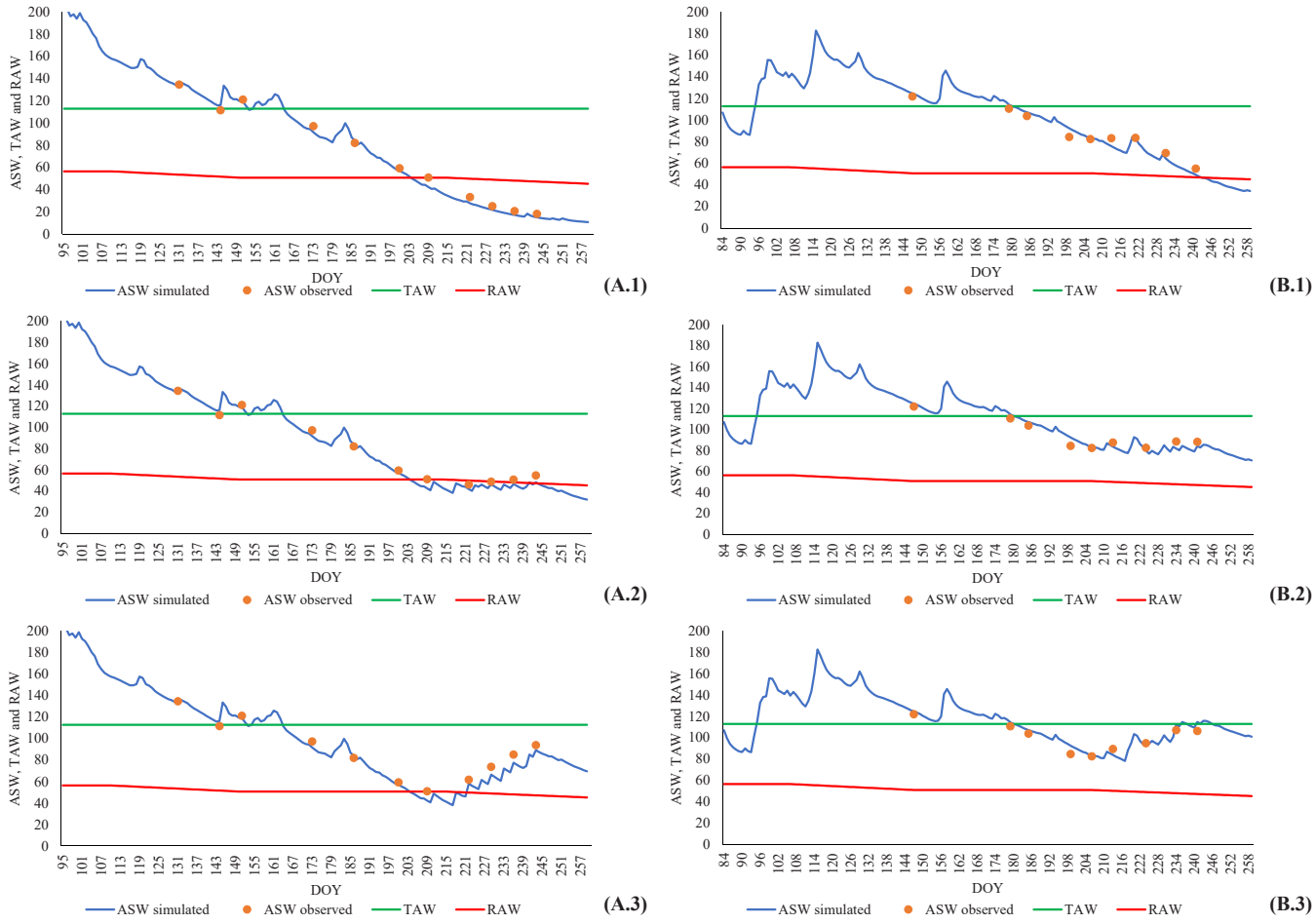

Fig. 2. Simulated (▬) vs. observed (●) average available soil water content (ASW) at 0.80-meter depth relative to (A) 2018 and (B) 2019. (1) Rainfed (R), (2) deficit irrigation (DI), (3) full irrigation (FI). TAW (▬) and RAW (▬) represent the total available and readily available soil water in the root zone, respectively. All values are expressed in mm.

Table 4
Goodness-of-fit indicators relative to the SIMDualKc model's calibration and validation for the different treatments in the 2018 and 2019 growing seasons.

	Year	2018			2019		
	Treatment	R	DI	FI	R	DI	FI
Linear regression	b	0.988	0.983	0.952	1.007	1.003	1.044
	r^2	0.995	0.993	0.980	0.971	0.928	0.963
Goodness-of-fit indicators	EF	0.989	0.979	0.932	0.938	0.887	0.839
	RMSE (mm)	4.320	4.557	5.384	4.845	4.500	5.267
	NRMSE (%)	6.302	5.848	6.684	5.488	4.764	5.148
	PBIAS (%)	3.377	3.233	5.386	0.025	−0.101	−4.503
	d_{IA}	0.997	0.995	0.984	0.987	0.989	0.961
	AAE (mm)	3.835	4.040	4.800	4.144	4.026	4.607

R: rainfed; DI: deficit irrigation; FI: full irrigation; b: regression coefficient, r^2: determination coefficient, EF: modelling efficiency; RMSE: root mean square error; NRMSE (%): normalized RMSE of total available water; PBIAS (%): percent bias of estimation; dIA: index of agreement; AAE: average absolute error (mm). The underlined data refer to the calibration results.

0.167) was greater than that in 2018 (ranging between 0.215 and 0.201). The most extreme values were reached in 2019.

During the 2018 and 2019 growth seasons, differences were observed in $K_{cb\ (gcover\ +\ crop)\ act}$ and K_e when comparing the same treatments (Table 5, Fig. 3). The maximum values for $K_{cb\ (gcover\ +\ crop)\ act}$ were obtained in the FI treatment. The DI treatment obtained the same values for $K_{cb\ (gcover\ +\ crop)\ act}$ as the FI treatment, with the exception of the end of the 2018 season, when the value was 0.03 lower. Treatment R had lower values than the other treatments in both years at the end of the season. The average K_e values were similar between the treatments and phenological states.

Regarding the crop and ground cover transpiration, differences were observed between the treatments at the end of the growing season (Fig. 5). This was likely due to the lower water availability during this growing season. In 2018, the values of this transpiration were lower in treatment R compared to the other treatments (Fig. 5 A). In 2019, the transpiration in treatment R was similar to that in the other treatments, with lower levels during the end of the season, due to the high precipitation that occurred during the 2019 season (Fig. 5 B).

A summary of all the crop water productivity parameters for both vineyards is presented in Table 6. The fruit yield and pruning wood values varied more between years than between treatments, verifying

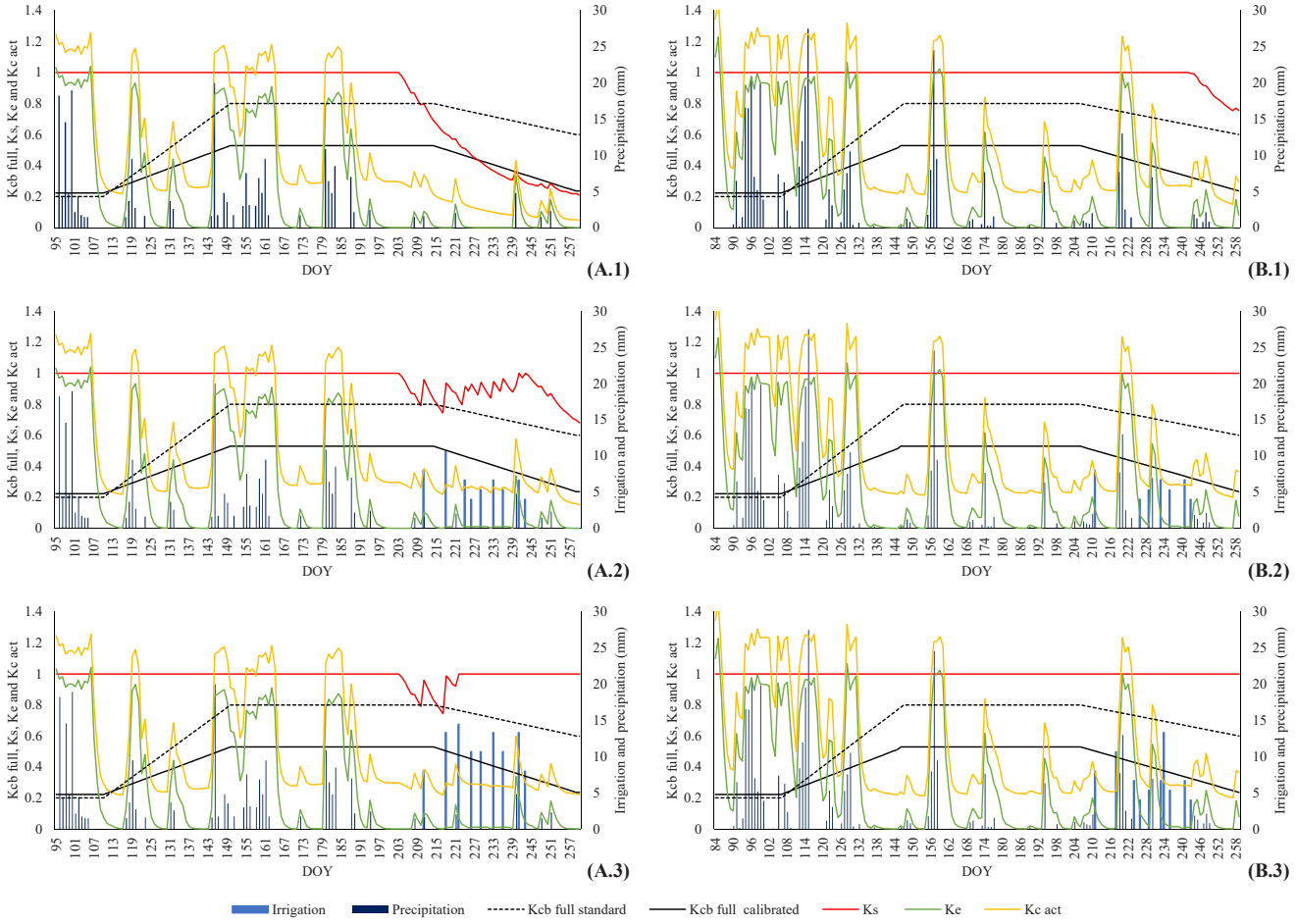

Fig. 3. Irrigation ( ), precipitation ( ), $K_{cb\ full}$ standard (--------), $K_{cb\ full}$ calibrated (——), K_s (——), K_e (——) and $K_{c\ act}$ (——) relative to (A) 2018 and (B) 2019. (1) Rainfed (R), (2), deficit irrigation (DI), (3) full irrigation (FI).

Table 5
Average values of crop coefficients and precipitation (mm) for different crop growth stages.

Crop Growth Stage	**2018**							
	DOY	$K_{cb\ (gcover\ +\ crop)\ act}$			K_e			Prec. (mm)
		R	DI	FI	R	DI	FI	
Initial	95–110	0.21	0.21	0.21	0.78	0.78	0.78	72
Rapid growth	110–150	0.24	0.24	0.24	0.27	0.27	0.27	57
Mid-season	150–214	0.28	0.28	0.28	0.29	0.29	0.29	88
End of season	214–260	0.10	0.23	0.26	0.03	0.04	0.04	11
	2019							
	DOY	$K_{cb\ (gcover\ +\ crop)\ act}$			K_e			Prec. (mm)
		R	DI	FI	R	DI	FI	
Initial	84–106	0.28	0.28	0.28	0.73	0.73	0.73	105
Rapid growth	106–147	0.26	0.26	0.26	0.41	0.41	0.41	111
Mid-season	147–206	0.22	0.22	0.22	0.17	0.17	0.17	66
End of season	206–259	0.23	0.24	0.24	0.16	0.16	0.16	45
Average 2018–2019		0.23	0.25	0.25	0.36	0.36	0.36	

$K_{cb\ (gcover\ +\ crop)\ act}$ = actual basal crop coefficient, K_e = soil evaporation coefficient, Prec. = precipitation (mm). R = rainfed, DI = deficit irrigation and FI = full irrigation treatment.

that, in 2018, the production of grapes and pruning wood was 2.3 and 1.9 times higher than in 2019, respectively. After conducting the univariate analysis of variance test, it was found that there was a significant difference between the years in terms of the fruit yield and pruning wood ($p < 0.001$). Regarding the WP results, in the first year of study, there were no significant differences between the treatments, although they were characterized by the highest yields and pruning wood levels. However, in the following year, most of the water productivity parameters showed statistically significant differences, indicating a trend towards deficit irrigation being the better treatment (Table 6). When considering the water productivity in terms of the transpiration and actual crop evapotranspiration, it was found that it was similar across all

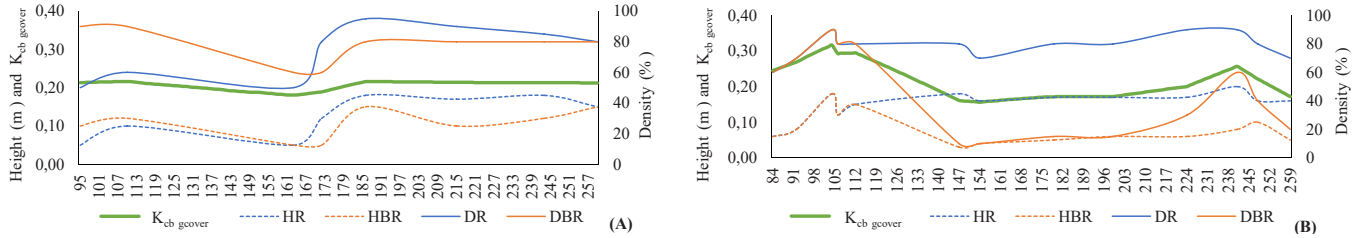

Fig. 4. Evolution of $K_{cb\ gcover}$ (—) (simulated by SIMDualKc) and active ground conditions: height (HR) (- - -), density in row (DR) (—), height (HBR) (- - -) and inter-row density (DBR) (—) relative to (A) 2018 and (B) 2019.

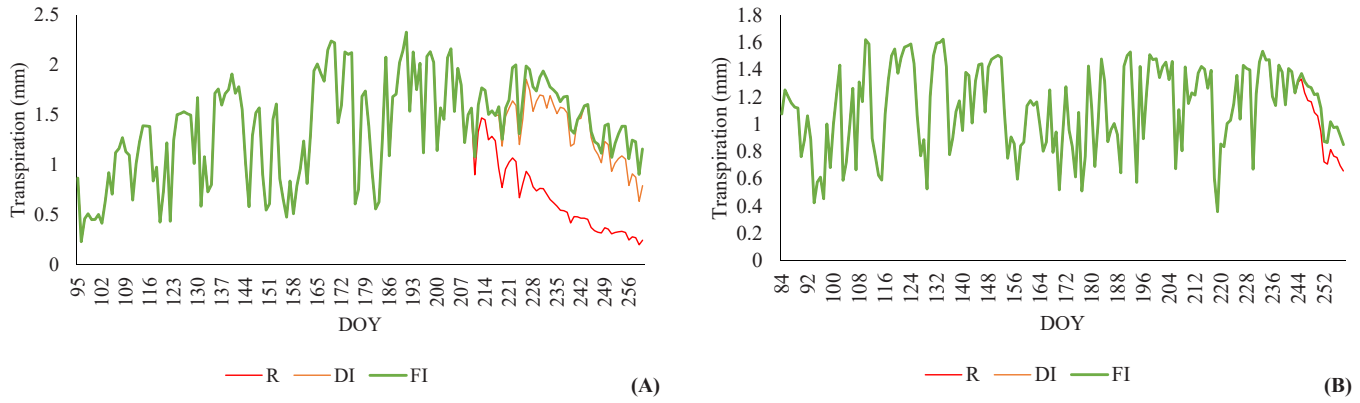

Fig. 5. Evolution of transpiration (crop plus ground cover) under R (—), DI(—) and FI (—) treatments relative to (A) 2018 and (B) 2019.

Table 6
Yield, pruning wood and water productivity indices under different irrigation treatments (R—rainfed, DI—deficit irrigation and FI—full irrigation) in 2018 and 2019.

Year	2018			2019		
Treatment	R	DI	FI	R	DI	FI
Yield (kg ha^{-1})	9700.02	11,236.60	10,146.60	3455.59^{b}	5024.74^{a}	5206.36^{ab}
Pruning wood (kg ha^{-1})	3276.92^{b}	3867.51^{ab}	4202.91^{a}	1695.39^{b}	2290.88^{a}	1838.71ab
WP_{FY} (kg m^{-3})	2.31	2.46	2.18	0.86^{b}	1.24^{ab}	1.28^{a}
WP_{PW} (kg m^{-3})	0.78	0.85	0.91	0.42^{ab}	0.57^{a}	0.45^{b}
WP_{FY+PW} (kg m^{-3})	3.09	3.31	3.09	1.29	1.81	1.73
WP_{T} (kg m^{-3})	5.23	5.09	4.45	1.77^{b}	2.55^{ab}	2.64^{a}
$WP_{ETc\ act}$ (kg m^{-3})	2.76	2.90	2.56	0.87^{b}	1.25^{ab}	1.30^{a}
WUE_{c} (-)	0.82	0.78	0.69	0.61	0.55	0.51

WP_{FY}: water productivity fruit yield, WP_{pw}: water productivity pruning wood, WP_{FY+PW}: sum of water productivity fruit yield and pruning wood, WP_{T}: water productivity referring to transpiration, $WP_{ETc\ act}$: water productivity referring to actual crop evapotranspiration, WUE_{c}: water use efficiency, R: rainfed, DI: deficit irrigation, FI: full irrigation, ΔASW: difference between ASW at initiation and harvest stages. For each variable, except WUE_{c}, lowercase letters compare different values within the year. Different letters indicate significant differences among groups with $p < 0.05$, using one-way ANOVA followed by Duncan's post hoc test.

treatments in 2018. However, significant differences were observed in 2019, where full irrigation presented the highest values, with differences compared to the control treatment but without significant differences in relation to deficit irrigation. Finally, in terms of WUE_{c} the highest values were obtained with the treatment with R, followed by the treatments with DI and FI in both years (Table 6).

4. Discussion

Differences in the calibrated $K_{cb\ full}$ and p values can be observed at the initial, mid- and end-season growth stages compared with the standard values (Table 3). These differences in the crop coefficients, particularly in the mid-season and at the end of the season, are attributed to factors such as the low plant density and the specific characteristics of the soil and climate for the Alvarinho cultivar, as previously reported by other authors (Kang et al., 2003). The canopy architecture and vine density, as suggested by Goodwin et al. (2006) and Ahmadi et al. (2019), can influence $K_{cb\ full}$. The lower values of $K_{cb\ full}$ observed in the present study may be justified by the significantly lower plant density used (1111 plant ha^{-1}) compared to other studies with cv. Loureiro (1666 plant ha^{-1}) (Silva et al., 2021), cv. Albariño (2222 plant ha^{-1}) (Fandiño et al., 2012) and cv. Tempranillo (2222 plant ha^{-1}) (López-Urrea et al., 2012). Furthermore, the lower height (h) and the fraction of soil covered by the crop in the vineyard (f_{c}) observed in this work, in comparison with other studies (Fandiño et al., 2012; Fandiño, 2021; Silva et al., 2021), resulting from the less vigorous plants and climatic conditions, may also have contributed to the lower $K_{cb\ full}$.

The best fit was achieved with equal or slightly higher p depletion fractions compared with the standard values (Table 3). The highest values of the p depletion fraction suggest that *Vitis vinifera* cv. Alvarinho is more tolerant to water stress than indicated in previous studies. The lowest $K_{cb\ mid}$ value to reduce the fraction of the soil surface covered by vegetation (f_{c}) was 0.41 (Pereira et al., 2023). The K_{cb} values obtained for the crop in this study were 0.17, 0.23 and 0.20 at the initial, mid-season and end-season, respectively. It was verified that all values are lower than those proposed for comparable climatic conditions

(Fandiño et al., 2012; Fandiño, 2021; Silva et al., 2021). Therefore, the value obtained in mid-season is lower than the value of 0.45 proposed by Pereira et al. (2023) for 'Low (diverse trellis and trainings), 2000–3300 pl/ ha', as well as that presented by Fandiño et al. (2012) (0.40) for cv. Alvariño with 2222 plant ha^{-1}. Furthermore, it was observed that this value exceeded the proposed value of 0.20 by Pereira et al. (2023) for the category 'Very low (young <5 years, diverse trellis, and training), 2000–3300pl/ha'. In this regard, despite the vineyard being over five years old, the K_{cb} values obtained for cv. Alvarinho is situated between the proposed values for the 'Very low' and 'Low' conditions (Pereira et al., 2023). This is attributable to a markedly reduced planting density, f_c and a diminished F_r value, with comparable conditions of heigh crop and M_L. This emphasises the necessity of providing detailed descriptions of the training system, density (number of vines per hectare) and f_c to facilitate the assessment of results across different locations, varieties and trellis systems.

A suitable approximation between the simulated and measured ASW values can be observed from Fig. 2. The model accurately predicted the ASW values in this work, as well as in other studies with different crops, climates and soils (Rolim et al., 2007; Paço et al., 2014; Paredes et al., 2018). However, the occasional overestimation or underestimation of the average was noted, as mentioned by Rosa et al. (2012a) and Paredes et al. (2018). Furthermore, it was observed that at the initial stages of both growth seasons, the available soil water (ASW) exceeded TAW. This can be attributed to the high precipitation that occurred prior and in the initiation stages, as illustrated in Fig. 1. The precipitation results in a high-water content in the soil. An examination of the data presented in Table 3, which concerns soil drainage, elucidates the elevated ASW values. In particular, the 'a' (400 mm) and 'b' values are associated with soil saturation and drainage speed, respectively. Furthermore, the minimal occurrence of surface runoff and deep percolation following precipitation contributed to the elevated ASW levels observed in subsequent periods. The elevated initial ASW in 2018 (Fig. 2 A) can be attributed to the 530 mm of precipitation (Fig. 1) that occurred prior to the initiation stage (DOY 1–95). In the 50 days following the initiation stage (up to DOY 145), precipitation levels reached 99 mm (Fig. 1), resulting in SIMDualKc consistently simulating values that exceeded TAW. In contrast, during the 2019 growing season, at the time of the initiation stage (DOY 84), the simulated ASW value was approaching the TAW (Fig. 2 B). The 219 mm of precipitation (significantly less than that recorded in 2018) recorded up to that point, in addition to the absence of precipitation 13 days before the initiation stage (Fig. 1), provide an explanation as to why the simulated ASW value was close TAW. However, in the subsequent 90-day period (up to DOY 174), precipitation levels reached 275 mm (Fig. 1), prompting SIMDualKc to simulate an ASW that exceeded the TAW (Fig. 2 B).

The regression to the origin demonstrated close agreement between the observed and simulated data (Table 4). Other indicators, such as the EF, RMSE, NRMSE, PBIAS, dIA and AAE, indicate that the prediction model, after calibration, efficiently estimated the ASW throughout the growing season with the different irrigation strategies. All indicators suggest that the model is suitable for use in different irrigation strategies (R, DI or FI) and years (2018 or 2019), emphasizing the robustness of the model.

The lower precipitation and higher temperature in 2018 (Fig. 1) also explain the lower ASW values in the R strategy in 2018 compared to R in 2019 (Fig. 1), resulting in longer periods of water stress (Fig. 3). This is especially evident in the $K_{c\ act}$ curve for the R strategy in 2018, the hottest year, which overall shows lower values compared to the same strategy in 2019 (Fig. 3). In 2018, the first irrigation event of the FI treatment occurred only 12 days after the onset of stress ($K_s<1$) and took 23 days to alleviate the water stress (Fig. 3). In contrast, in 2019, there was no water stress in the FI and DI strategies. These differences can be attributed to variations in precipitation (Table 5) and ET_o (Fig. 1) between the two study years.

The irrigation treatments started and ended on the same DOY in both years. However, during the growing season of 2018, the FI and DI strategies received 28 mm and 17 mm more, respectively, than during the growing season of 2019. Despite the higher amounts of irrigation recorded in 2018, they were not sufficient to prevent water stress, as stress periods were observed in all treatments, including FI (Fig. 3). The occurrence of water stress periods can be identified through $K_s<1$ (Fig. 3) and when the ASW > RAW (Fig. 2). In the R treatments (Fig. 3 A1, Fig. 3 B1), after the water stress started ($K_s < 1$), there was no recovery until the end of the growing season. However, in the DI treatments (Fig. 3 A2, Fig. 3 B2), the stress periods were shorter in 2019 (only at the end of the growing season), and, in both years, they were also shorter in duration due to irrigation events compensating for the water shortages. In 2019, in the FI treatments (Fig. 3 B3), there were no water stress periods. In 2018 FI, periods of $K_s<1$ were observed, primarily influenced by climatic factors (Fig. 1); however, $K_s=1$ was restored when irrigation began (Fig. 3 B3). No differences were observed in K_s, K_e and $K_{c\ act}$ between the DI and FI treatments in 2019. This lack of difference was attributed to the precipitation that occurred at the end of the growing season. In 2018, there was greater water stress during this period due to low precipitation. Furthermore, during the initial growth stages (Fig. 3), there were moments when the K_e values closely approached the $K_{c\ act}$, reaching 1.2. This can be interpreted as a result of the high rainfall that occurred during these stages, even in the absence of ground cover vegetation (Fig. 4). This evolution in the K_e and K_c values has been observed by other authors for other *Vitis vinifera* crops, namely 'Godello' and 'Mencía' (Cancela et al., 2015) and Loureiro (Silva et al., 2021).

In analysing the results of $K_{cb\ (gcover\ +\ crop)\ act}$ for the three treatments across two seasons (Table 5), a reduction in their potential values is evident, particularly in the R and DI treatments, during the mid-season and the end of the season. The $K_{cb\ (gcover\ +\ crop)\ act}$ values during the initial stage (0.21 in 2018 and 0.28 in 2019) were lower than the values reported by previous authors (≈ 0.60) (Yunusa et al., 1997; Fandiño et al., 2012). However, at this stage, no differences between the treatments were observed, as the initial conditions were the same. The values achieved for $K_{cb\ (gcover\ +\ crop)\ act}$ (0.22 and 0.28 in 2019 and 2018, respectively) in the mid-season were lower than those presented by Silva et al. (2021), who reported a value of 0.42 for this period.

During the mid-season, the values obtained for $K_{cb\ (gcover\ +\ crop)\ act}$ (0.22 in 2019 and 0.28 in 2018) were lower than those presented by (Silva et al., 2021), who reported values of 0.42 for this period. This difference in $K_{cb\ (gcover\ +\ crop)\ act}$ is justified by variations in the conditions of the vineyard; for example, the height (2.4 m) and the density of the plant reported for cv. Loureiro (1666 plant ha^{-1}) were greater than in our study (height 1.8 m and density 1111 plant ha^{-1}). In contrast, at the end of the season, slightly lower mean values of $K_{cb\ (gcover\ +\ crop)\ act}$ were obtained for the FI and DI treatments (≈ 0.24) compared to the mean values reported by Fandiño et al. (2012) and Silva et al. (2021), who reported $K_{cb\ (gcover\ +\ crop)\ act}$ values of 0.30 and 0.41, respectively. However, as shown in Rallo et al. (2021), lower plant densities are associated with a lower K_{cb}.

The fruit yield and pruning wood values showed more significant variations between years than between treatments. In 2018, the production of grapes and pruning wood was significantly higher ($p<0.001$) than in 2019 (Table 6). These parameters are influenced by the weather conditions, such as precipitation and evapotranspiration (Lisek, 2008; González-Fernández et al., 2020). Despite the higher total precipitation recorded in 2019 (328 mm) compared to 2018 (227 mm), a substantial portion of this precipitation occurred during periods of lower water requirements (initial and rapid growth). In contrast, during the mid-season, when the water requirements were higher, the precipitation was higher in 2018, contributing to the observed differences in the yield (kg ha^{-1}) and pruning wood (kg ha^{-1}). The evapotranspiration did not differ notably between the growing seasons or crop growth stages (Fig. 1), with 882 mm and 814 mm recorded in 2018 and 2019, respectively, evenly distributed across the different crop growth stages.

During the growing seasons, it was observed that the crop and ground cover transpiration treatments exhibited variations at the end of the growing season. These differences were attributed to water stress and were more evident in 2018 due to increased periods of stress.

The SimDualKc software was used to determine the water required to achieve the FY, the transpiration (crop plus ground cover, $m^3\ ha^{-1}$) and the actual crop evapotranspiration ($m^3\ ha^{-1}$) involved in the different treatments during the two growing seasons. The integration of the model's results in Eqs. 20 to 25 aids in understanding the water productivity (WP) and crop water use efficiency (WUE_c). Regarding the WP results (Table 6), it was observed that when considering variations in ASW between the beginning and end of the growing season, the DI strategy consistently yielded the best results in the three WP indices, regardless of the year; this indicates that this strategy represents the most balanced approach to water usage in relation to production. However, regarding the WP_{FY} index for 2019, the results for the FI strategy were higher than those obtained with DI, although not to a statistically significant degree ($p>0.05$) (Table 6). In this context, the year with the lowest fruit yield (2019) demonstrates that the FI strategy is more efficient in terms of water usage in grape production in this WP_{GY} when compared to the R treatment ($p<0.05$). This observation aligns with findings for other grapevine varieties, such as Godello and Treixadura (Trigo-Córdoba et al., 2015), where the water productivity values were slightly higher in treatments that incorporated some level of water stress. The WP values reported in the present study were higher than those reported for Godello and Treixadura, indicating that more water is needed to produce one kilogram of Alvarinho grapes. However, the WP values for the Alvarinho cultivar in this study were similar to those reported in a previous study (Cancela et al., 2016), as well as for the Perlette and Superior varieties (Er-Raki et al., 2021). This study concludes that the irrigation deficit strategy demonstrates the most effective water use, which is why this approach should be adopted for this cultivar.

The water productivity values obtained in this study, which referred to the transpiration and actual crop evapotranspiration, varied significantly between the years. However, our values for 2018 were higher than those obtained by Er-Raki et al., (2021), although they were lower in 2019. In 2019, our values were similar to or greater than those obtained in semiarid climate conditions (Teixeira et al., 2007). In contrast, compared with the values obtained by Fandiño (2021), in the Albariño variety arranged in '*Parral*', our values for WP_T and WP_{ETc} were lower, by approximately half. In a similar manner, Phogat et al. (2017) obtained higher values for Chardonnay in Australia. The deficit irrigation strategy showed a positive effect on the yield (+3.6 %) and WP_{ETc} (+4.7 %), contrary to Wen et al. (2023) in vine fruit, where there was a decrease of 9.0 % in the yield in a deficit irrigation strategy, although with an increase of 9.9 % in WP_{ETc}, double that obtained in the Albariño case. Finally, in terms of WUE_c, values lower than 1 were obtained for all treatments. These values are in agreement with the WUE_c values (0.63–0.91) observed in a proximal area to cv. Albariño (Fandiño, 2021).

The water productivity (WP) and crop water use efficiency (WUE_c) values may be improved without a cover crop. This is because the transpiration of the cover crop and its contribution to the evapotranspiration of the current crop, as well as its water consumption, were not considered. However, some authors have reported that the water use by active ground cover is environmentally sustainable when considering the numerous ecosystem services provided by cover crops in vineyards (Lopes et al., 2011; Garcia et al., 2018; Gattullo et al., 2020). These results demonstrate the importance of vineyard management and the local climatic conditions, as factors that allow for adequate comparisons between results. The use of water productivity and water use efficiency indices based on transpiration and/or actual crop evapotranspiration is highlighted as a useful tool to manage irrigation in vineyards in temperate climates. Moreover, water savings in irrigation could be obtained, increasing the WP and WUEc, although it is necessary to include the yield and grape quality effects (Chen et al., 2023).

5. Conclusions

In this study, two useful tools for sustainable water management were combined. Through SimDualKc, the dynamics of the evolution of the water in the soil and the subsequent transpiration (T) (crop plus ground cover, $m^3\ ha^{-1}$) and $ET_{c\ act}$ (actual crop evapotranspiration, $m^3\ ha^{-1}$) were obtained. These results, when combined with the fruit and pruning yields, demonstrate that the strategy of deficit irrigation is the one that brings the most production and environmental advantages. The current study demonstrated the successful performance of the SIMDualKc model for *Vitis vinifera* cv. Alvarinho, considering specific parameters related to the soil, climate, crop stage and irrigation observed in the present work. Adjustments were made to the standard values (Allen et al., 1998) for the 2018 R treatment, resulting in an accurate approximation between the observed and simulated values. The study concludes, in line with the findings of other authors, that the model can correctly predict the ASW. These accurately predicted values can significantly contribute to improved irrigation management throughout the growth season, allowing farmers to improve their water management practices. For practical application, it is recommended to round the values of the basal crop coefficient to 0.15, 0.25 and 0.20 at the beginning, middle and end of the season, respectively. These values are suitable to similar vineyard agronomic conditions with lower vine density and fc, and presence of active ground cover. Regarding water productivity, a significant advantage was observed when employing a deficit irrigation strategy, as it consistently yielded the best WP values in both years. The water extracted from the soil represents a significant portion of the total water consumed by the crop and cover crop during the growing season and therefore must be included in the WP calculations. Incorporating this aspect reduces the differences in WP between treatments, but the most efficient strategy remains deficit irrigation. Given the climate uncertainty that affects this location, with drier summers, the adoption of irrigation systems improves and stabilizes the WP. Conversely, further studies should focus on the economic efficiency related to the installation of irrigation systems in this region. The findings highlight the need for additional studies involving other grapevine cultivars, given the observed high variability in crop coefficients even within similar cultivars, as evidenced by the differences between the studied cultivar and cv. Loureiro (Silva et al., 2021) and cv. Albariño (Fandiño et al., 2012). In future studies, it would be beneficial to incorporate both methodologies to study other varieties of *Vitis vinifera* and under different climatic conditions, as well as to incorporate data from other sources, such as transpiration from sap flow measurements or from lysimeters. Our study was conducted over a two-year period, which may be a limitation in terms of accurately representing crop growing seasons, given the significant climatic differences between the two years. A further limitation of the study is that only 28 production values were obtained for each irrigation strategy in each year, and these were the only values taken into account when calculating the WP. It could therefore be beneficial to analyse more than two years (growing seasons) and a greater number of plants to obtain more robust results.

CRediT authorship contribution statement

Susana Mendes: Writing – review & editing, Validation. **Claúdio Araujo-Paredes:** Writing – review & editing, Data curation. **Simão P. Silva:** Writing – review & editing, Writing – original draft, Validation, Software, Methodology, Investigation, Formal analysis, Data curation. **M. Isabel Valín:** Writing – review & editing, Validation, Investigation, Formal analysis, Data curation, Conceptualization. **Javier J Cancela:** Writing – review & editing, Software, Methodology, Conceptualization.

Declaration of Competing Interest

The authors declare the following financial interests/personal relationships which may be considered as potential competing interests. M Isabel Valin reports equipment, drugs, or supplies was provided by Foundation for Science and Technology. Susana Mendes reports equipment, drugs, or supplies was provided by Foundation for Science and Technology. Claudio Araujo-Paredes reports equipment, drugs, or supplies was provided by Foundation for Science and Technology. Javier J Cancela reports article publishing charges was provided by Consellería de Cultura, Educación e Universidade, Xunta de Galicia. If there are other authors, they declare that they have no known competing financial interests or personal relationships that could have appeared to influence the work reported in this paper.

Data Availability

Data will be made available on request.

Acknowledgements

This work was supported by project UIDB/05937/2020 — Center for Research and Development in Agrifood Systems and Sustainability (CISAS), through national funds from the Foundation for Science and Technology, and Project UIDP/05975/2020, proMetheus—Research Unit on Energy, Materials and Environment for Sustainability. The APC was funded by Consellería de Cultura, Educación e Universidade, Xunta de Galicia (Grupos de Referencia Competitiva ED431C-2021–27), to Jorge Dafonte and María Fandiño, in relation to an ECa study. The authors are grateful to the editors and the anonymous reviewers for their insightful comments and suggestions.

Appendix A. Nomenclature

ASW	available soil water (mm)
DBR	active ground cover density in inter-row area (%)
DI	deficit irrigation
DOY	day of year
DR	active ground cover density in row (%)
$ET_{c\ act}$	actual crop evapotranspiration (mm day^{-1})
ET_o	reference evapotranspiration (mm day^{-1})
f_c	fraction of soil shaded by crop
F_r	stomatal adjustment
FI	full irrigation
GCV	ground cover vegetation
FY	vineyard fruit yield (kg ha^{-1})
h	crop height measured from soil (m)
HBR	active ground cover height in inter-row area (m)
HR	active ground cover height in row (m)
$K_{c\ act}$	crop coefficient adjusted to climate and local conditions
K_{cb}	basal crop coefficient
$K_{cb\ (gcover\ +\ crop)\ act}$	basal crop and active ground cover coefficient adjusted to climate and actual conditions
$K_{cb\ act}$	actual crop coefficient
$K_{cb\ crop}$	main crop basal crop coefficient
$K_{cb\ full\ end}$	end full basal crop coefficient
$K_{cb\ full\ ini}$	initial full basal crop coefficient
$K_{cb\ full\ mid}$	mid-season full basal crop coefficient
$K_{cb\ gcover}$	ground cover crop coefficient
K_e	soil evaporation coefficient
K_s	stress coefficient
M_L	canopy transparency
p	depletion fraction for no stress
Prec.	precipitation (mm)
PW	pruning wood (kg ha^{-1})
R	rainfed
RAW	readily available soil water (mm)
REW	readily evaporable water (mm)
T	crop and ground cover transpiration (m^3 ha^{-1})
TAW	total available soil water (mm)
TEW	total evaporable water (mm)
TWU	total water use (m^3 ha^{-1})
WP	water productivity (kg m^{-3})
WUE_c	crop water use efficiency (-)
Z_e	depth of evaporable layer

Appendix B. Density and height of cover crop in row and inter-row areas in 2018 and 2019 growing seasons

Year	Day of year	Density in rows (%)	Density between rows (%)	Height in rows (m)	Height between rows (m)	Baggiolini scale (Baggiolini et al., 1993)
2018	95	50	90	0.05	0.10	C
	110	60	90	0.10	0.12	D
	163	50	60	0.05	0.05	I
	172	80	60	0.12	0.05	K

(*continued on next page*)

(*continued*)

Year	Day of year	Density in rows (%)	Density between rows (%)	Height in rows (m)	Height between rows (m)	Baggiolini scale (Baggiolini et al., 1993)
	186	95	80	0.18	0.15	L
	215	90	80	0.17	0.1	M
	243	85	80	0.18	0.12	M
	260	80	80	0.15	0.15	N
2019	84	60	60	0.06	0.06	C
	92	70	70	0.08	0.08	C
	104	90	90	0.18	0.18	C
	106	80	80	0.12	0.12	C
	112	80	80	0.15	0.15	D
	147	80	10	0.18	0.03	I
	154	70	10	0.16	0.04	J
	179	80	15	0.17	0.05	K
	199	80	15	0.17	0.06	L
	224	90	30	0.17	0.06	M
	241	90	60	0.20	0.08	M
	248	80	40	0.16	0.10	M
	259	70	20	0.16	0.05	N

Appendix C. Location and apparent electrical conductivity

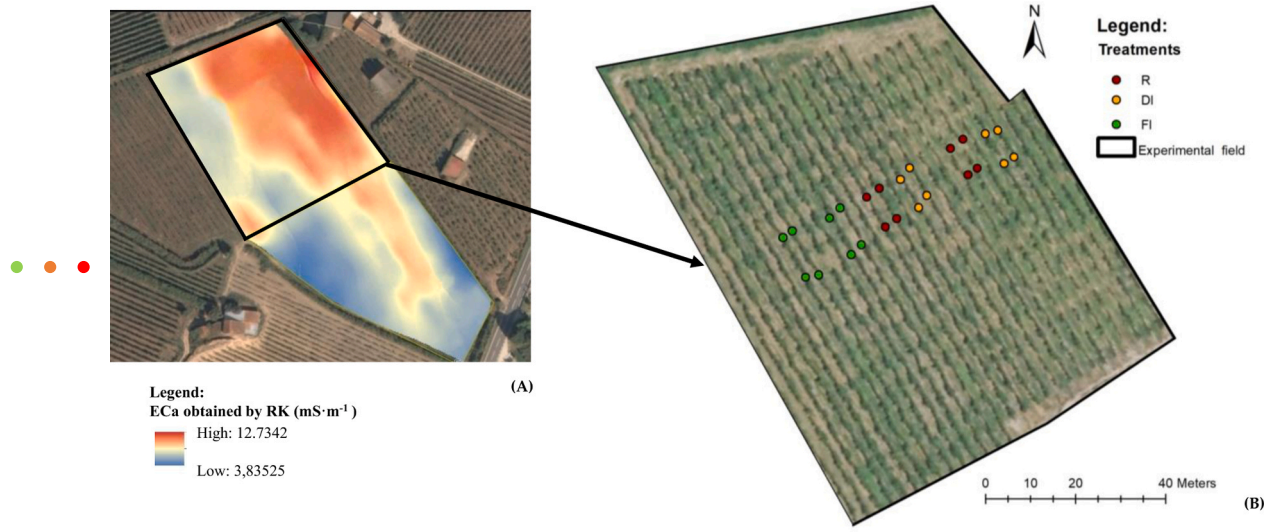

Fig. C.1. Study area. A: Soil electrical conductivity apparent (ECa) map obtained by RK (mS·m-1). B: Positions of access probe tubes located in full irrigation (), deficit irrigation () and rainfed () treatments.

Appendix D. Experimental design of each repetition: locations of plants, drippers and access probe tubes

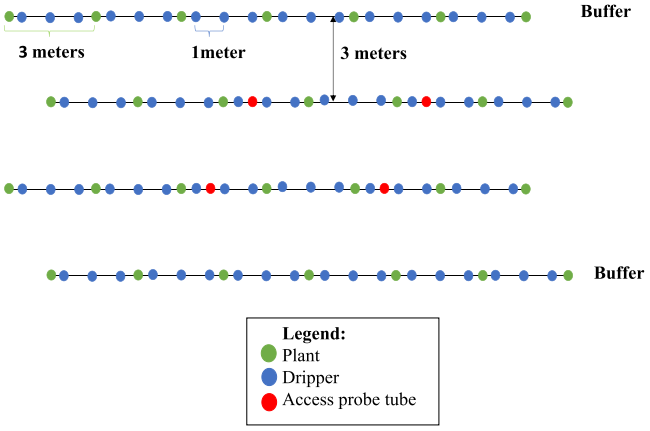

Fig. D.1. Spatial locations of plants, drippers and access probe tubes.

References

Acevedo-Opazo, C., Ortega-Farias, S., Fuentes, S., 2010. Effects of grapevine (Vitis vinifera L.) water status on water consumption, vegetative growth and grape quality: an irrigation scheduling application to achieve regulated deficit irrigation. Agric. Water Manag 97, 956–964. https://doi.org/10.1016/j.agwat.2010.01.025.

Afonso, J.M., Monteiro, A.M., Lopes, C.M., Lourenço, J., 2003. Cover cropping at "Vinhos Verdes" wine region. A three year study in variety 'Alvarinho.'. Cienc. e Tec. Vitivinic. V. 18.

Ahmadi, S.H., Solgi, S., Sepaskhah, A.R., 2019. Quinoa: A super or pseudo-super crop? Evidences from evapotranspiration, root growth, crop coefficients, and water productivity in a hot and semi-arid area under three planting densities. Agric. Water Manag 225, 105784. https://doi.org/10.1016/j.agwat.2019.105784.

Alcamo, J., Flörke, M., Märker, M., 2007. Future long-term changes in global water resources driven by socio-economic and climatic changes. Hydrol. Sci. J. 52, 247–275. https://doi.org/10.1623/hysj.52.2.247.

Allen, R.G., 1996. Assessing Integrity of Weather Data for Reference Evapotranspiration Estimation. J. Irrig. Drain. Eng. 122, 97–106. https://doi.org/10.1061/(asce)0733-9437(1996)122:2(97).

Allen, R.G., Pereira, L.S., 2009. Estimating crop coefficients from fraction of ground cover and height. Irrig. Sci. 28, 17–34. https://doi.org/10.1007/s00271-009-0182-z.

Allen, R.G., Pereira, L.S., Smith, M., Raes, D., 1998. Crop Evapotranspiration. Guidelines for Computing Crop Water Requirements. FAO Irrig. Drain. Pap. 56, 300.

Allen, R.G., Pereira, L.S., Howell, T.A., Jensen, M.E., 2011. Evapotranspiration information reporting: I. Factors governing measurement accuracy. Agric. Water Manag 98, 899–920. https://doi.org/10.1016/j.agwat.2010.12.015.

Araújo-Paredes, C., Portela, F., Mendes, S., Valín, M.I., 2022. Using Aerial Thermal Imagery to Evaluate Water Status in Vitis vinifera cv. Loureiro. Sensors 22. https://doi.org/10.3390/s22208056.

Baggiolini, M., Lorenz, H., Bleiholder, H., et al., 1993. Stades phénologiques repères de la vigne. Arboric. Hortic. 44, 7–9.

Beyá-Marshall, V., Arcos, E., Seguel, Ó., et al., 2022. Optimal irrigation management for avocado (cv. 'Hass') trees by monitoring soil water content and plant water status. Agric. Water Manag 271. https://doi.org/10.1016/j.agwat.2022.107794.

Brown, I., Poggio, L., Gimona, A., Castellazzi, M., 2011. Climate change, drought risk and land capability for agriculture: Implications for land use in Scotland. Reg. Environ. Chang 11, 503–518. https://doi.org/10.1007/s10113-010-0163-z.

Buesa, I., Pérez, D., Castel, J., et al., 2017. Effect of deficit irrigation on vine performance and grape composition of Vitis vinifera L. cv. Muscat of Alexandria. Aust. J. Grape Wine Res 23, 251–259. https://doi.org/10.1111/ajgw.12280.

Bwambale, E., Abagale, F.K., Anornu, G.K., 2022. Smart irrigation monitoring and control strategies for improving water use efficiency in precision agriculture: A review. Agric. Water Manag 260, 107324. https://doi.org/10.1016/j.agwat.2021.107324.

Cancela, J.J., Fandiño, M., Rey, B.J., Martínez, E.M., 2015. Automatic irrigation system based on dual crop coefficient, soil and plant water status for Vitis vinifera (cv Godello and cv Mencía). Agric. Water Manag 151, 52–63. https://doi.org/10.1016/j.agwat.2014.10.020.

Cancela, J.J., Trigo-Córdoba, E., Martínez, E.M., et al., 2016. Effects of climate variability on irrigation scheduling in white varieties of Vitis vinifera (L.) of NW Spain. Agric. Water Manag 170, 99–109. https://doi.org/10.1016/j.agwat.2016.01.004.

Chen, V., Khan, T.A., Chiavaroli, L., et al., 2023. Response to comment on "Relation of fruit juice with adiposity and diabetes depends on how fruit juice is defined: a re-analysis of the EFSA draft scientific opinion on the tolerable upper intake level for dietary sugars" by Chen et al. 2023. Eur. J. Clin. Nutr. 77, 1178–1179. https://doi.org/10.1038/s41430-023-01323-6.

Civit, B., Piastrellini, R., Curadelli, S., Arena, A.P., 2018. The water consumed in the production of grapes for vinification (Vitis vinifera). Mapping the blue and green water footprint. Ecol. Indic. 85, 236–243. https://doi.org/10.1016/j.ecolind.2017.10.037.

Darouich, H., Karfoul, R., Ramos, T.B., Pereira, L.S., 2023. Setting Irrigation Thresholds for Building a Platform Aimed at the Improved Management of Citrus Orchards in Coastal Syria. Agronomy 13. https://doi.org/10.3390/agronomy13071794.

Djaman, K., O'Neill, M., Owen, C.K., et al., 2018. Crop evapotranspiration, irrigation water requirement and water productivity of maize from meteorological data under semiarid climate. Water (Switz.) 10. https://doi.org/10.3390/w10040405.

El-Sadek, A., 2014. Water use optimisation based on the concept of Partial Rootzone Drying. Ain Shams Eng. J. 5, 55–62. https://doi.org/10.1016/j.asej.2013.09.004.

Er-Raki, S., Bouras, E., Rodriguez, J.C., et al., 2021. Parameterization of the AquaCrop model for simulating table grapes growth and water productivity in an arid region of Mexico. Agric. Water Manag 245, 106585. https://doi.org/10.1016/j.agwat.2020.106585.

Evett, S.R., Stone, K.C., Schwartz, R.C., et al., 2019. Resolving discrepancies between laboratory-determined field capacity values and field water content observations: implications for irrigation management. Irrig. Sci. 37, 751–759. https://doi.org/10.1007/s00271-019-00644-4.

Fandiño, M., 2021. Necesidades de Agua e influencia de los sistemas de riego en Vitis vinifera var. Escuela De Doctorado Internacional De La Universidad De Santiago De Compostela, Albariño.

Fandiño, M., Cancela, J.J., Rey, B.J., et al., 2012. Using the dual-K c approach to model evapotranspiration of Albariño vineyards (Vitis vinifera L. cv. Albariño) with consideration of active ground cover. Agric. Water Manag 112, 75–87. https://doi.org/10.1016/j.agwat.2012.06.008.

FAO & WWC (2015) Towards a Water and Food Secure Future. White Pap 61.

Fatichi S., Paschalis A., Bonetti S., et al (2023) Water use efficiency: A review of spatial and temporal variability. In: Goss MJ, Oliver MBT-E of S in the E (Second E (eds). Academic Press, Oxford, pp 527–542.

Fernández, E., 2023. Editorial note on terms for crop evapotranspiration, water use efficiency and water productivity. Agric. Water Manag 289, 2021–2023. https://doi.org/10.1016/j.agwat.2023.108548.

Fernández, J.E., Alcon, F., Diaz-Espejo, A., et al., 2020. Water use indicators and economic analysis for on-farm irrigation decision: A case study of a super high density olive tree orchard. Agric. Water Manag 237, 106074. https://doi.org/10.1016/j.agwat.2020.106074.

Fischer, G., Tubiello, F.N., van Velthuizen, H., Wiberg, D.A., 2007. Climate change impacts on irrigation water requirements: Effects of mitigation, 1990-2080. Technol. Forecast Soc. Change 74, 1083–1107. https://doi.org/10.1016/j.techfore.2006.05.021.

Fraga, H., Malheiro, A.C., Moutinho-Pereira, J., Santos, J.A., 2014. Climate factors driving wine production in the Portuguese Minho region. Agric. Meteor. 185, 26–36. https://doi.org/10.1016/j.agrformet.2013.11.003.

Garcia, L., Celette, F., Gary, C., et al., 2018. Management of service crops for the provision of ecosystem services in vineyards: A review. Agric. Ecosyst. Environ. 251, 158–170. https://doi.org/10.1016/j.agee.2017.09.030.

Gattullo, C.E., Mezzapesa, G.N., Stellacci, A.M., et al., 2020. Cover crop for a sustainable viticulture: Effects on soil properties and table grape production. Agronomy 10. https://doi.org/10.3390/agronomy10091334.

González Perea, R., Daccache, A., Rodríguez Díaz, J.A., et al., 2018. Modelling impacts of precision irrigation on crop yield and in-field water management. Precis Agric. 19, 497–512. https://doi.org/10.1007/s11119-017-9535-4.

Gonzalez-Fernandez, E., Pina-Rey, A., Fernandez-Gonzalez, M., et al., 2020. Prediction of Grapevine Yield Based on Reproductive Variables and the Influence of Meteorological Conditions. Agron.-BASEL 10. https://doi.org/10.3390/agronomy10050714.

Goodwin, I., Whitfield, D.M., Connor, D.J., 2006. Effects of tree size on water use of peach (Prunus persica L. Batsch). Irrig. Sci. 24, 59–68. https://doi.org/10.1007/s00271-005-0010-z.

Iglesias, A., Garrote, L., 2015. Adaptation strategies for agricultural water management under climate change in Europe. Agric. Water Manag 155, 113–124. https://doi.org/10.1016/j.agwat.2015.03.014.

Jiang, X., He, L., 2021. Investigation of effective irrigation strategies for high-density apple orchards in pennsylvania. Agronomy 11. https://doi.org/10.3390/agronomy11040732.

Junquera, P., Lissarrague, J.R., Jiménez, L., et al., 2012. Long-term effects of different irrigation strategies on yield components, vine vigour, and grape composition in cv. Cabernet-Sauvignon (Vitis vinifera L.). Irrig. Sci. 30, 351–361. https://doi.org/10.1007/s00271-012-0348-y.

Kang, S., Gu, B., Du, T., Zhang, J., 2003. Crop coefficient and ratio of transpiration to evapotranspiration of winter wheat and maize in a semi-humid region. Agric. Water Manag 59, 239–254. https://doi.org/10.1016/S0378-3774(02)00150-6.

Kottek, M., Grieser, J., Beck, C., et al., 2006. World map of the Köppen-Geiger climate classification updated. Meteor. Z. 15, 259–263. https://doi.org/10.1127/0941-2948/2006/0130.

KPMG International (2012) Expect the Unexpected: Building business value ina changing world: Executive Summmary. 1–20.

Lakso, A.N., Santiago, M., Stroock, A.D., 2022. Monitoring Stem Water Potential with an Embedded Microtensiometer to Inform Irrigation Scheduling in Fruit Crops. Horticulturae 8. https://doi.org/10.3390/horticulturae8121207.

Lisek, J., 2008. Climatic factors affecting development and yielding of grapevine in central Poland. J. Fruit. Ornam. Plant Res 16, 285–293.

Liu, Y., Pereira, L.S., Fernando, R.M., 2006. Fluxes through the bottom boundary of the root zone in silty soils: Parametric approaches to estimate groundwater contribution and percolation. Agric. Water Manag 84, 27–40. https://doi.org/10.1016/j.agwat.2006.01.018.

Lopes, C.M., Santos, T.P., Monteiro, A., et al., 2011. Combining cover cropping with deficit irrigation in a Mediterranean low vigor vineyard. Sci. Hortic. (Amst.) 129, 603–612. https://doi.org/10.1016/j.scienta.2011.04.033.

López-Urrea, R., Montoro, A., Mañas, F., et al., 2012. Evapotranspiration and crop coefficients from lysimeter measurements of mature "Tempranillo" wine grapes. Agric. Water Manag 112, 13–20. https://doi.org/10.1016/j.agwat.2012.05.009.

Ma, X., Han, F., Wu, J., et al., 2023. Optimizing crop water productivity and altering root distribution of Chardonnay grapevine (Vitis vinifera L.) in a silt loam soil through direct root-zone deficit irrigation. Agric. Water Manag 277, 108072. https://doi.org/10.1016/j.agwat.2022.108072.

Merriam J.L., Keller J. (1978) Farm irrigation system evaluation: A guide for management. 211:271.

Mirás-Avalos, J.M., Cancela, J.J., Fandiño, M., et al., 2020. Zoning of a newly-planted vineyard: Spatial variability of physico-chemical soil properties. Soil Syst. 4, 1–17. https://doi.org/10.3390/soilsystems4040062.

Nadler, A., 1982. Estimating the soil water dependence of the electrical conductivity soil solution/electric conductivity bulk soil ratio [Soil salinity]. J. Soil Sci. Soc. Am. V. 46.

Paço, T.A., Pôças, I., Cunha, M., et al., 2014. Evapotranspiration and crop coefficients for a super intensive olive orchard. An application of SIMDualKc and METRIC models using ground and satellite observations. J. Hydrol. 519, 2067–2080. https://doi.org/10.1016/j.jhydrol.2014.09.075.

Pagay, V., 2022. Evaluating a novel microtensiometer for continuous trunk water potential measurements in field-grown irrigated grapevines. Irrig. Sci. 40, 45–54. https://doi.org/10.1007/s00271-021-00758-8.

Paredes, P., Rodrigues, G.J., Petry, M.T., et al., 2018. Evapotranspiration partition and crop coefficients of Tifton 85 bermudagrass as affected by the frequency of cuttings. Application of the FAO56 dual Kc model. Water (Switz.) 10. https://doi.org/10.3390/w10050558.

Pereira, L.S., Paredes, P., Jovanovic, N., 2020a. Soil water balance models for determining crop water and irrigation requirements and irrigation scheduling focusing on the FAO56 method and the dual Kc approach. Agric. Water Manag 241, 106357. https://doi.org/10.1016/j.agwat.2020.106357.

Pereira, L.S., Paredes, P., Melton, F., et al., 2020b. Prediction of crop coefficients from fraction of ground cover and height. Background and validation using ground and remote sensing data. Agric. Water Manag 241, 106197. https://doi.org/10.1016/j.agwat.2020.106197.

Pereira, L.S., Paredes, P., Hunsaker, D.J., et al., 2021. a) Updates and advances to the FAO56 crop water requirements method. Agric. Water Manag 248. https://doi.org/10.1016/j.agwat.2020.106697.

Pereira, L.S., Paredes, P., Melton, F., et al., 2021b. Prediction of crop coefficients from fraction of ground cover and height: Practical application to vegetable, field and fruit crops with focus on parameterization. Agric. Water Manag 252, 106663. https://doi.org/10.1016/j.agwat.2020.106663.

Pereira, L.S., Paredes, P., Montoya, F., et al., 2023. Single and basal crop coefficients for estimation of water use of tree and vine woody crops with consideration of fraction of ground cover, height, and training system. 3. Tropical and subtropical fruit crops. Irrig. Sci. https://doi.org/10.1007/s00271-023-00901-7.

Phogat, V., Skewes, M.A., McCarthy, M.G., et al., 2017. Evaluation of crop coefficients, water productivity, and water balance components for wine grapes irrigated at different deficit levels by a sub-surface drip. Agric. Water Manag 180, 22–34. https://doi.org/10.1016/j.agwat.2016.10.016.

Prieto, J.A., Louarn, G., Perez Peña, J., et al., 2020. A functional-structural plant model that simulates whole- canopy gas exchange of grapevine plants (Vitis vinifera L.) under different training systems. Ann. Bot. 126, 647–660. https://doi.org/10.1093/aob/mcz203.

Ragab, R., 2002. A holistic generic integrated approach for irrigation, crop and field management: The SALTMED model. Environ. Model Softw. 17, 345–361. https://doi.org/10.1016/S1364-8152(01)00079-2.

Rallo, G., Paço, T.A., Paredes, P., et al., 2021. Updated single and dual crop coefficients for tree and vine fruit crops. Agric. Water Manag 250, 106645. https://doi.org/10.1016/j.agwat.2020.106645.

Rodrigues, G.C., Pereira, L.S., 2009. Assessing economic impacts of deficit irrigation as related to water productivity and water costs. Biosyst. Eng. 103, 536–551. https://doi.org/10.1016/j.biosystemseng.2009.05.002.

Rolim, J., Godinho, P., Sequeira, B., et al., 2007. Assessing the SIMDualKc model for irrigation scheduling simulation in Mediterranean environments. Water Sav. Mediterr. Agric. Futur Res needs I 49–61.

Rosa, R.D., Paredes, P., Rodrigues, G.C., et al., 2012b. Implementing the dual crop coefficient approach in interactive software. 1. Background and computational strategy. Agric. Water Manag 103, 8–24. https://doi.org/10.1016/j.agwat.2011.10.013.

Rosa, R.D., Paredes, P., Rodrigues, G.C., et al., 2012a. Implementing the dual crop coefficient approach in interactive software: 2. Model testing. Agric. Water Manag 103, 62–77. https://doi.org/10.1016/j.agwat.2011.10.018.

Shellie, K.C., 2014. Water productivity, yield, and berry composition in sustained versus regulated deficit irrigation of merlot grapevines. Am. J. Enol. Vitic. 65, 197–205. https://doi.org/10.5344/ajev.2014.13112.

Silva, S.P., Valín, M.I., Mendes, S., et al., 2021. Dual Crop Coefficient Approach in Vitis vinifera L. cv. Loureiro. Agronomy 11, 2062. https://doi.org/10.3390/agronomy11102062.

Soltekin, O., Teker, T., Altındişli, A., 2020. Deficit irrigation strategies in Vitis vinifera L. 'Crimson Seedless' table grape: physiological responses, growth, yield and fruit quality. Acta Hortic. 1276, 197–204. https://doi.org/10.17660/ActaHortic.2020.1276.28.

Teixeira, A.H. d C., Bastiaanssen WGM, Bassoi, L.H., 2007. Crop water parameters of irrigated wine and table grapes to support water productivity analysis in the São Francisco river basin, Brazil. Agric. Water Manag 94, 31–42. https://doi.org/10.1016/j.agwat.2007.08.001.

Trigo-Córdoba, E., Bouzas-Cid, Y., Orriols-Fernández, I., Mirás-Avalos, J.M., 2015. Effects of deficit irrigation on the performance of grapevine (Vitis vinifera L.) cv. "Godello" and "Treixadura" in Ribeiro, NW Spain. Agric. Water Manag 161, 20–30. https://doi.org/10.1016/j.agwat.2015.07.011.

Trout, T.J., DeJonge, K.C., 2017. Water productivity of maize in the US high plains. Irrig. Sci. 35, 251–266. https://doi.org/10.1007/s00271-017-0540-1.

Wen, S., Cui, N., Gong, D., et al., 2023. A global meta-analysis of yield and water productivity of woody, herbaceous and vine fruits under deficit irrigation. Agric. Water Manag 287, 108412. https://doi.org/10.1016/j.agwat.2023.108412.

Yunusa, I.A.M., Walker, R.R., Guy, J.R., 1997. Partitioning of seasonal evapotranspiration from a commercial furrow-irrigated Sultana vineyard. Irrig. Sci. 18, 45–54. https://doi.org/10.1007/s002710050043.

Yuste, J., Rubio, J.A., Pérez, M.A., 2004. Influence of plant density and water regime on soil water use, water relations and productivity of trellis-trained Tempranillo grapevines. Acta Hortic. 646, 187–193. https://doi.org/10.17660/ActaHortic.2004.646.24.

Zhang, S., Wang, H., Sun, X., et al., 2021. Effects of farming practices on yield and crop water productivity of wheat, maize and potato in China: a meta-analysis. Agric. Water Manag 243, 106444. https://doi.org/10.1016/j.agwat.2020.106444.

Zhou H., Ma L., Zhang S., et al (2023) Effect of Water-Fertilizer Coupling on the Growth and Physiological Characteristics of Young Apple Trees.